



HAL
open science

Aircraft Wake Vortex Study and Characterization with 1.5 μm Fiber Doppler Lidar

A. Dolfi-Bouteyre, B. Augere, M. Valla, D. Goular, D. Fleury, G. Canat, C. Planchat, T. Gaudo, C. Besson, A. Gilliot, et al.

► **To cite this version:**

A. Dolfi-Bouteyre, B. Augere, M. Valla, D. Goular, D. Fleury, et al.. Aircraft Wake Vortex Study and Characterization with 1.5 μm Fiber Doppler Lidar. Aerospace Lab, 2009, 1, p. 1-13. hal-01180652

HAL Id: hal-01180652

<https://hal.science/hal-01180652>

Submitted on 27 Jul 2015

HAL is a multi-disciplinary open access archive for the deposit and dissemination of scientific research documents, whether they are published or not. The documents may come from teaching and research institutions in France or abroad, or from public or private research centers.

L'archive ouverte pluridisciplinaire **HAL**, est destinée au dépôt et à la diffusion de documents scientifiques de niveau recherche, publiés ou non, émanant des établissements d'enseignement et de recherche français ou étrangers, des laboratoires publics ou privés.

A. Dolfi-Bouteyre, B. Augere,
M. Valla, D. Goular, D. Fleury,
G. Canat, C. Planchat, T. Gaudo,
C. Besson, A. Gilliot (Onera)
J.-P. Cariou, O. Petilon,
J. Lawson-Daku (Leosphere)
S. Brousmiche, S. Lugan,
L. Bricteux, B. Macq
(Université catholique de Louvain)

E-mail: Agnes.Dolfi-Bouteyre@onera.fr

Aircraft Wake Vortex Study and Characterization with 1.5 μm Fiber Doppler Lidar

For ten years now, Onera has been developing lidar tools for wake vortex detection and studies. Since 2003, new developments based on 1.5 μm fibered laser sources have been achieved in parallel with extensive research work on the laser sources themselves. Three innovative lidars have been developed and are presented in this paper:

- 1) A mini-lidar, based on a CW (continuous-wave) 2 W / 1.5 μm laser source, for aircraft model wake vortex characterization in a catapult facility. A self-triangulation technique allows the vortex core position to be found with 10 cm error, and the circulation error is 10 %.
- 2) A pulsed 1.5 μm lidar, based on a 50 μJ / 15 kHz MOPA (Master Oscillator Power Amplifier) source, for lateral wake vortex monitoring at airports. The range is 400 m, the core position error is about ± 2 m and the circulation error is about 10 %.
- 3) A pulsed 1.5 μm lidar, based on a 120 μJ / 12 kHz MOPA source, for onboard axial wake vortex detection. Ground based lidar tests at Orly airport have demonstrated wake vortex detection up to 1.2 km.

Introduction

Detecting atmospheric hazards such as wind shear, clear air turbulence and wake vortices has been a major concern for twenty years. The lift force exerted on the aircraft wing creates a counter-rotating pair of trailing vortices (wake vortex) which constitute a potential hazard to following aircraft. Detecting these vortices is of crucial importance for flight safety, airport capacity and aircraft design [1].

The experimental techniques used to study wake vortices include coherent lidar (light detection and ranging), also called coherent laser radar or CLR. Coherent lidars are practical and efficient tools to characterize and monitor wind fields and more specifically wake vortices [2], [3], [4]. The measurement of the Doppler shift of light (from a laser source), after scattering from atmospheric particles, implies the line-of-sight flow velocity and allows a picture of vortex flow to be built up. Monitoring of vortices at ranges exceeding a few hundred meters is best carried out using pulsed lidar. Detailed measurements at short range are better obtained with CW (continuous-wave) lidar [5]. Lidars have the potential to help with low-vortex wing design and for quantifying the vortex hazard from existing aircraft.

Because low-vortex wing design requires extended measurements, reduced-scale test facilities such as wind tunnels, water tanks or catapults have been used to perform easy and low-cost measurements. Full-scale measurements are however necessary to check the atmospheric impact on wake vortex evolution and lidar is the link between reduced-scale and full-scale approaches.

Onera has been developing these coherent detection lidar tools for wake vortex characterization and monitoring for ten years now. New developments are based on 1.5 μm fiber laser sources, which have a high electrical to optical efficiency ~ 10 %, thus allowing for low electrical consumption. This wavelength is also the most favorable for eyesafe lidar designs: as the maximum laser energy imposed by eye safety regulations is high, the laser power can be increased with little constraint on the lidar operation or design. It is now well-established that a fiber architecture is easy to adjust and mechanically reliable in a vibrating environment; other advantages are the compactness and flexibility in terms of onboard installation. The lidar can be split into subsystems, far apart in the aircraft body and linked by fiber optics. 1.5 μm fiber coherent lidars have recently been flown with success [5], [6].

In this paper we will present the most recent lidar developments at Onera for wake vortex characterization and monitoring. The coherent detection lidar technique and architecture are first described. Then we present reduced-scale measurements with a self-triangulation CW technique. The measurements are compared with PIV (particle imaging velocimetry) for ground-based tests (Box 1). The rest of this article deals with full-scale measurements at airport sites with pulsed lidar. The lidar developed for transverse wake vortex measurements is presented. Finally, we describe a future onboard pulsed lidar for axial wake vortex detection based on a high-brightness large-core fiber amplifier (Box 2: comparison between full-scale and reduced-scale measurements).

Coherent detection lidar principle and wake vortex detection application

Coherent detection lidar principle

Accurate distant wind velocity measurements are possible with laser anemometry based on coherent detection lidar (Figure 1). A laser beam is focused on atmospheric aerosols, and then reflected by Mie diffusion. The reflected beam is frequency shifted because of relative displacement between the aerosols and the lidar (the Doppler effect). In order to measure the radial velocity information contained in the beam phase, the backscattered beam is mixed in an optical interferometer with a reference beam (the LO or local oscillator). Thanks to a close optical frequency match between the backscattered beam and the LO, this coherent beam combining allows for a convenient transposition into the radiofrequency domain. The electric current given by the optical detection (the so-called heterodyne current) is described by:

$$i_{het}(t) = \sqrt{2 \cdot K \cdot P_s \cdot P_{LO}} \cdot \cos(2\pi(f_s - f_{LO} + f_D)t + \phi) \quad (1)$$

where K is a coefficient taking into account heterodyne efficiency and detector efficiency, P_s is the backscattered beam power, P_{LO} is the local oscillator beam power, f_s is the laser source frequency, f_{LO} is the local oscillator frequency, ϕ is the heterodyne signal phase, f_D is the

Doppler frequency given by $f_D = \frac{2 \cdot V_r}{\lambda}$ where V_r is the radial velocity,

and λ is the laser beam wavelength. The shift f_D is 1.3 MHz per m/s for a laser wavelength of $1.54 \mu\text{m}$.

In practice, the LO beam is additionally shifted (via an acousto-optic modulator) by typically $F = 40 \text{ MHz}$ or 70 MHz , depending on the application. The heterodyne signal frequency is then $f_s - f_{LO} + f_D = \Delta f + f_D$. Moreover, the term $\sqrt{2 \cdot K \cdot P_s \cdot P_{LO}}$ in the heterodyne current shows that coherent detection enhances the detection sensibility by multiplying the very weak backscattered signal power by the local oscillator power.

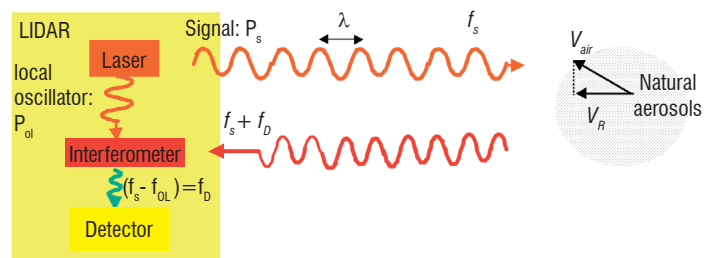


Figure 1 - Coherent detection lidar principle.

Wake vortex characterization

An aircraft in flight always creates vortices in its wake, and their strength increases with the mass of the aircraft. In a plane perpendicular to the aircraft path, the largest vortices are generated at the wingtips. These are large masses of rotating air with induced tangential velocities as high as 30 m/s.

In order to characterize wake vortices with a lidar, a scanning device is used as shown in Figure 2.

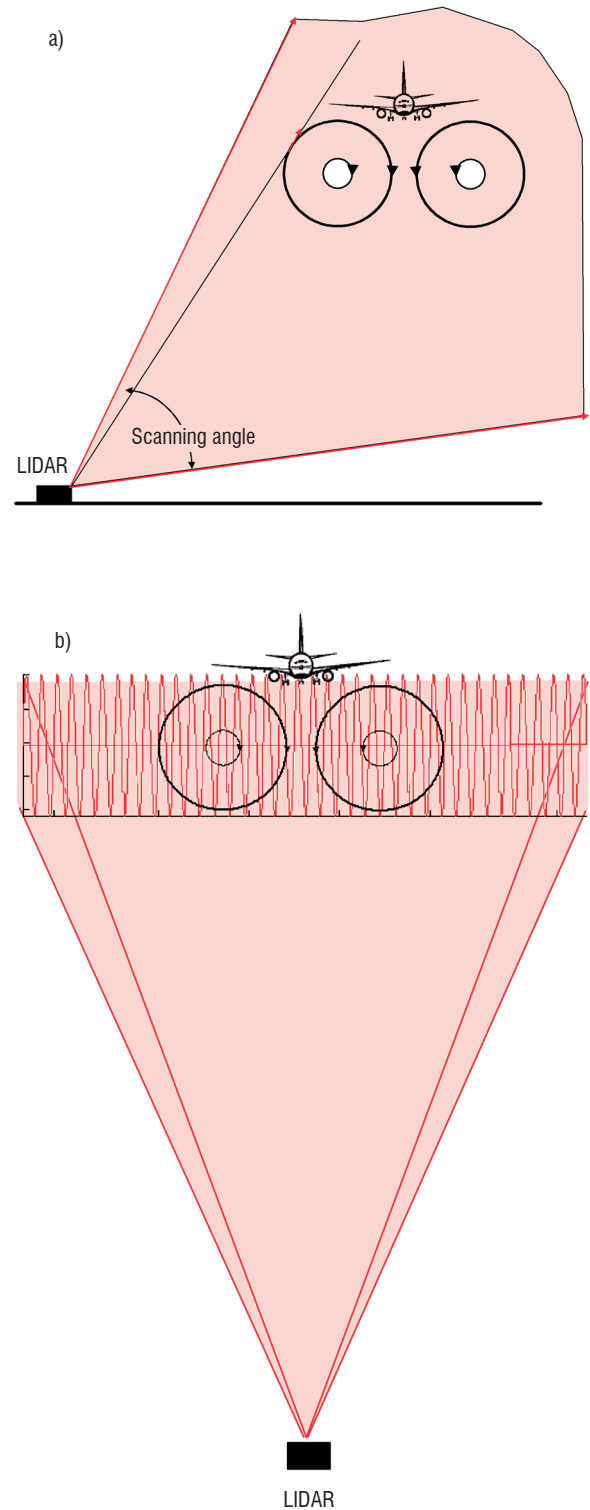


Figure 2 - Lidar scanning pattern: (a) for lateral wake vortex detection, (b) for axial wake vortex detection.

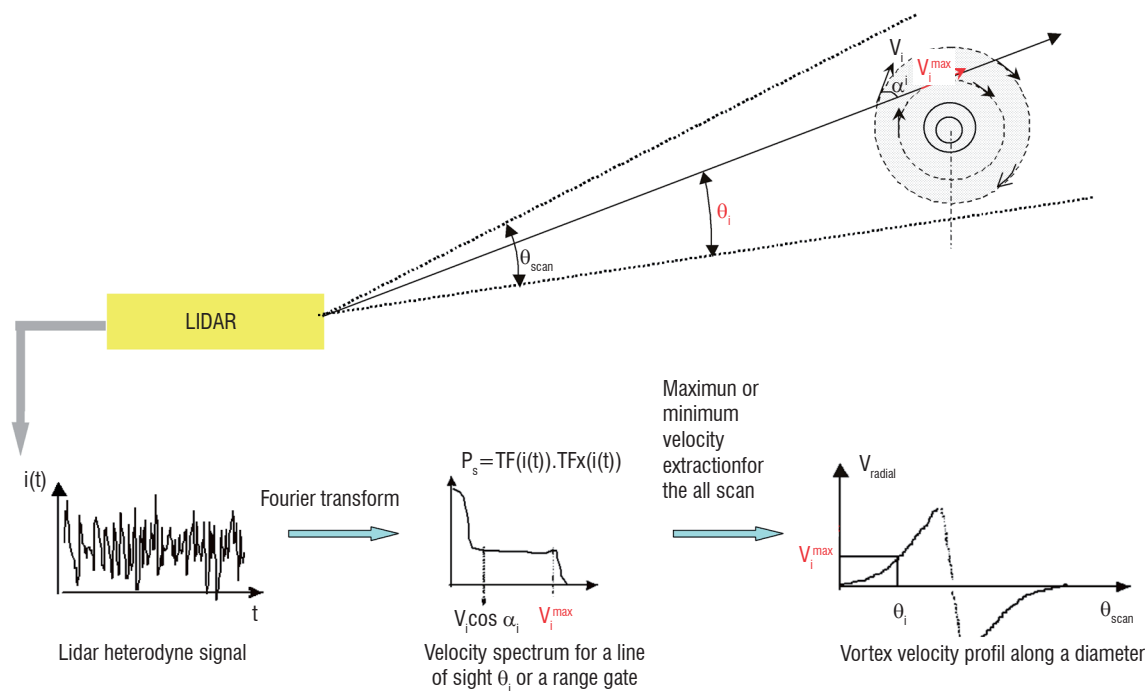


Figure 3 - Signal processing scheme for lidar lateral characterization of a vortex.

Lateral detection and characterization

For lateral detection, the scan is in a plane perpendicular to the aircraft path (Figure 2a) so the measured tangential velocities are very high. The signal processing usually associated with this lateral (side-ways on) detection is detailed in Figure 3. A Fourier-transform power spectral estimate for the heterodyne signal yields a weighted velocity distribution (weighted along the whole line of sight for CW lidar, or within the range gate for pulsed lidar). For a scan angle θ_i the highest velocity measured (in absolute value) is the tangential one shown as V_i^{max} . The maximum (or minimum) velocity extraction for each line of sight or range gate enables us to reconstruct the velocity profile along a diameter of the wake vortex.

Axial detection

A pulsed laser allows the wind field to be spatially resolved along its line of sight, and scanning of the laser (e.g. the sinusoidal scan of Figure 2b) allows for the generation of an accurate 3D velocity image of the wind field.

Wake vortex axial detection is more difficult because the radial velocity components (the projections of the 3D air velocity on the lidar beam axis) are very low. Instead of radial velocity, it is easier to detect the spectral broadening due to vortex turbulence.

Reduced-scale measurements

The Onera catapult facility offers the possibility of observing the total lifetime of the wake, starting from its origin at the wing, up to about a hundred wingspans. In this facility, non-motorized free-flying scale models are propelled by means of a pneumatic catapult via a trolley. Once launched, the model flies freely without any wall or mounting interference in a 90 m long, 20 m wide and 20 m high observation area. Afterwards, the model is recovered from a volume of plastic foam (Figure 4). Reduced-scale aircraft models have wingspans in the 2 m range (Figure 5).

Oil droplets are generated to seed the vortices. Lidar measurements in vertical observation planes, transverse to the flight path of the model,

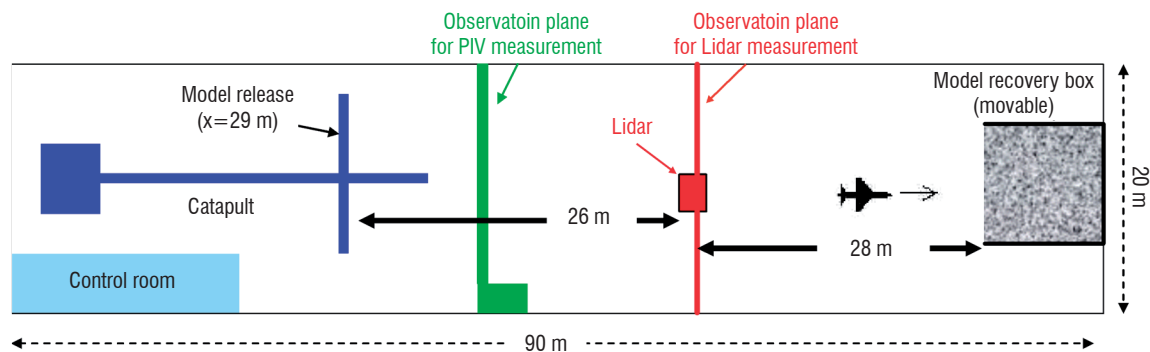


Figure 4 - B20 catapult facility (view from above): observation planes for PIV and lidar measurements.

allow for tracking of the wake vortex development, giving a precise description of the secondary flow field as well as of the velocity profiles. Because the phenomena to be analyzed are small, a CW lidar is used. But with a single CW lidar, only angular vortex core positions can be derived. Triangulation has proved a successful way to characterize full-scale wake vortices with 2 CW lidars [7]. An innovative setup for the mini-lidar was developed by Onera in order to apply the triangulation method and thus obtain the vortex trajectory as a function of time (or of distance up to ~ 100 spans). In this autonomous (self-triangulation) configuration, a second beam scanner was added to investigate the same wind field from an offset viewpoint (Figure 6). It is therefore possible to determine the positions of the cores and their trajectories over time. The scanning is carried out sequentially on each scanner with a measurement rate of 1.25 Hz (period of 0.4 s for each scanner).

The accuracy of the core location depends on the triangulation base length (distance between the two scanners), and on the angular measurement accuracy (dependent on the number of spectra averaged). Our base length is around 5 m and the precision of the core positions is better than 10 cm.

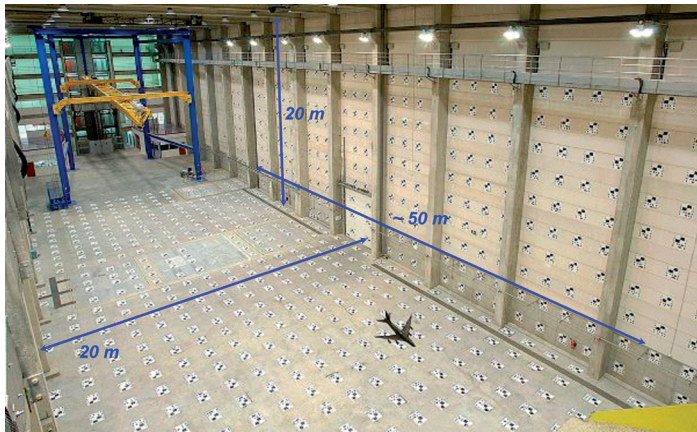
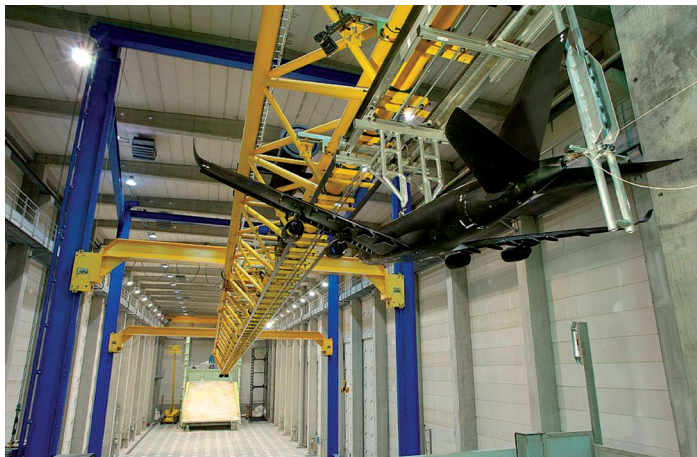


Figure 5 - B20 catapult facility with a very large transport aircraft model.

The mini-lidar has a 2W CW $1.5 \mu\text{m}$ laser, an aperture diameter of 20 mm, and a measurement depth (given by the weighting along the line of sight) of 2 m at 8 m height.

Figure 7 shows an example of vortex velocity spectra viewed alternatively from scanner 1 (circle a) and from scanner 2 (circle b). The horizontal axis is the time after over flight (or the scanning angle), the vertical axis is the velocity, and the color scale gives the power spectral density. The vortex velocity profiles are extracted from those images as explained in Figure 3 and are drawn in white. Core posi-

tions are extracted automatically from the derivative of these profiles. Then a value of circulation (m^2/s , related to the vortex strength) is calculated.

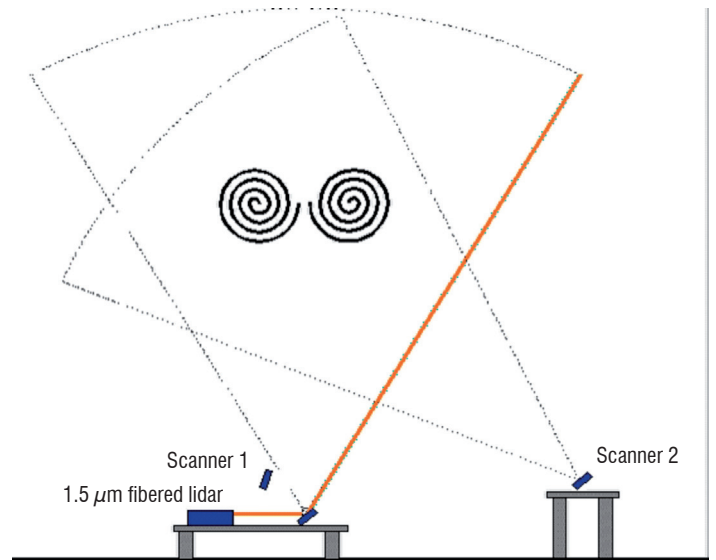


Figure 6 - Mini-lidar in self-triangulation configuration.

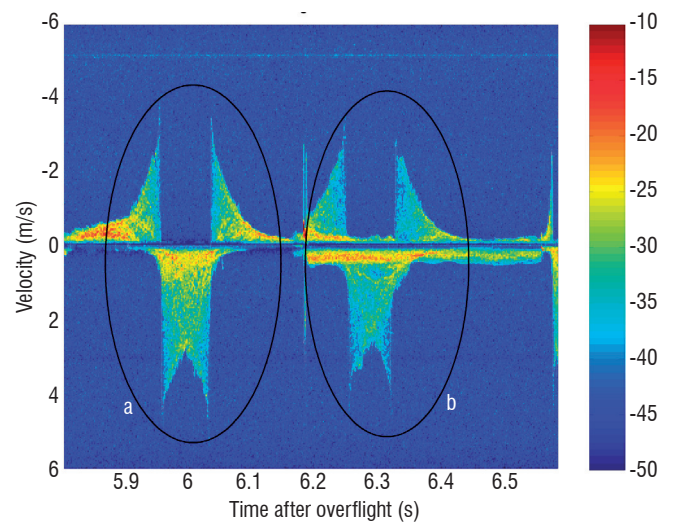


Figure 7 - Vortex velocity spectra: (circle a) viewed from scanner 1, (circle b) viewed from scanner 2). (Horizontal axis) time after over flight. (Vertical axis) velocity (m/s).

Figure 8 gives an example of measurement results: a) vortices' positions in the measurement plane with an accuracy of 10 cm in each direction; b) the circulation values as functions of wingspan.

Wingspan units are equivalent to time units (number of wingspans = time after overflight x aircraft model velocity) and allow for the easiest comparisons between reduced-scale measurements and full-scale measurements (see Box 2).

In addition to lidar measurements, PIV is performed simultaneously to analyze the vortices. PIV (particle imaging velocimetry) gives the 2D wind field perpendicular to the trajectory [16]. PIV and lidar measurements were performed on two different observation planes (Figure 4). However, they are complementary, since the first method allowed for detailed characterizations of the wake flow to ~ 40 wing spans behind the model, while the second ones tracked the vortices up to ~ 100 spans. PIV allows for measurements of multipolar structures in the near field whereas

lidar is more useful when there is only one vortex in the far field. Measurement adequacy was demonstrated and the data provide mutual support for result interpretation. Comparisons between PIV measurements and lidar measurements are presented in Box 1. Using lidar in a catapult facility is a cheap and easy way to perform extensive studies for low-vortex wing design. However full-scale measurements are mandatory to study the atmospheric impact.

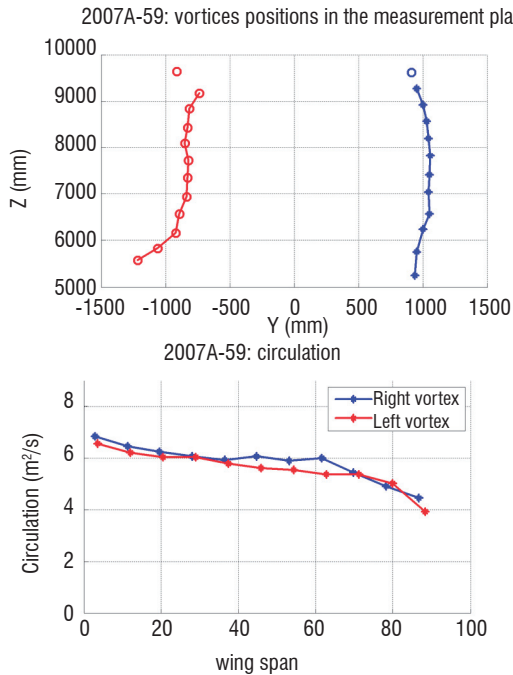


Figure 8 - (a) Example of descending vortex trajectory in the measurement plan, (b) circulation values as functions of wingspan.

Lateral full-scale wake vortex measurements

For wake-vortex lateral full-scale measurement purposes, various systems have been developed using CO₂ [7] and HoTm: YAG sources [9]. Onera has developed the first eye safe pulsed fiber lidar for wake vortex monitoring and characterization. Its design is based on a 1.5 μm fiber laser and high power telecom components. This new lidar was installed at Frankfurt airport field in February and March 2007 in order to perform wake vortex measurements for aircraft departures as part of the CREDOS EU project.

The lidar is composed of three innovative sub-systems: a pulsed fiber laser based on a Master Oscillator Power Fiber Amplifier (MOPFA) architecture, a compact Brewster circulator, and a user-friendly human-machine interface (HMI) with real-time wake vortex monitoring. The MOPFA architecture allows the pulse duration, shape and repetition rate to be optimized for lidar applications. For wake vortex detection, a pulse duration of 250 ns was chosen as a trade off between velocity resolution and spatial resolution.

The main characteristics of Onera's wake vortex lidar (SWAN) are:

- Wavelength: 1.55 μm
- Range: 400 m
- Min distance: 50 m
- Longitudinal resolution: 2.4 m after signal processing
- Lateral resolution: 3 mrad (1 m at 300 m)
- Speed resolution: 1 m/s
- Frame rate: ~0.25 Hz for a scanning angle range of 60°

- Fibered polarization-maintaining (PM) laser 50 μJ / 15 kHz designed and built at Onera
- Fibered PM architecture
- Real time velocity field signal processing and display.
- Eye safety

Figure 9 gives a schematic view of the lidar design. Figure 10 shows the optical architecture.

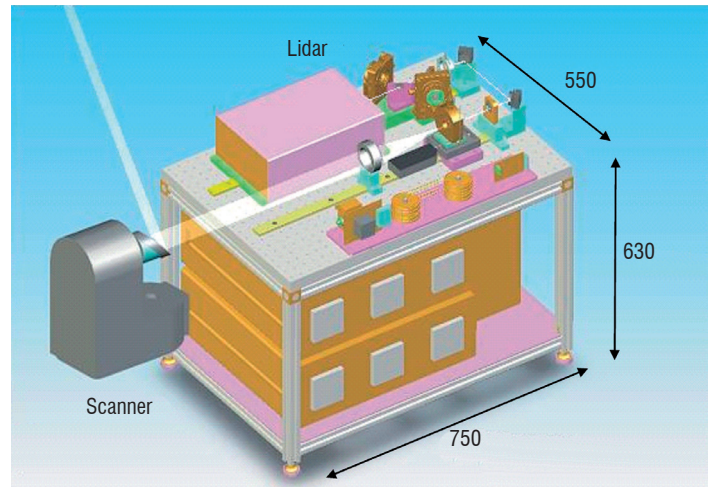


Figure 9 - Drawing and size of SWAN lidar.

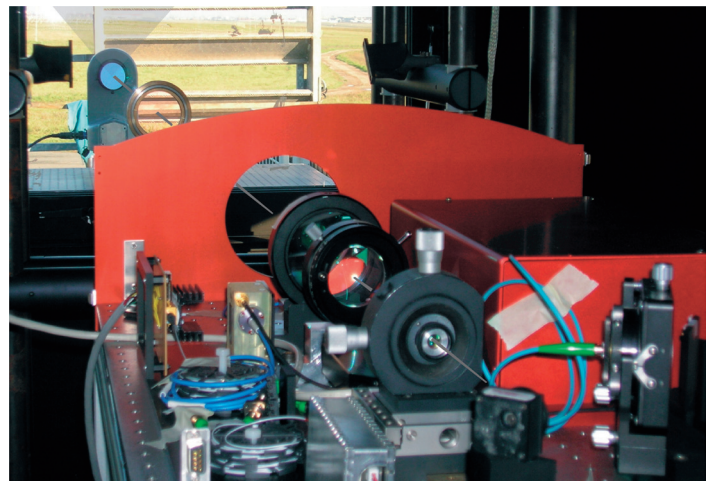


Figure 10 - Picture of lidar optical design.

Laser

The MOPFA using Erbium-Ytterbium doped fibers is well-suited for 1.5 μm high energy pulse generation. The peak power is however limited by stimulated Brillouin scattering (SBS) because of the narrow spectral linewidth. To overcome this limitation, large-mode-area (LMA) fibers are required [8]. These fibers must also have low core numerical apertures to avoid multimode operation and minimize amplified spontaneous emission (ASE). We recently developed a 3-stage all-fiber amplifier. The third amplification stage is built with a large core fiber which guides up to 6 LP mode groups. Thanks to proper packaging, the beam quality is still compatible with coherent detection requirements (the beam quality factor M² was measured to be close to 1.3). The beam is better than 98 % linearly polarized. With an 8 W pump power source, pulse repetition frequencies (PRFs) of 15 kHz have been reached, allowing hundreds of lidar signals to be averaged on each line of sight and thus significantly reducing the speckle noise.

Optical architecture

The optical architecture is based on collimated beams, and can thus be used with different fiber lasers, even with multimode fibers, as the laser output is collimated in free space. A compact circulator has been specially designed with both robustness and very good optical isolation (60 dB). The output beam has an effective Gaussian diameter of 50 mm (at $1/e^2$ intensity, with $M^2 = 1.3$), allowing a focus range up to 300 m. The received beam is focused on a single mode PM fiber before being mixed with the fibered local oscillator. The LO beam is frequency shifted by $f = 70$ MHz before being injected into the amplifier, allowing the sign of the Doppler shift to be measured (see § Coherent detection lidar principle, page 5).

Signal processing and display

In order to display the wake vortex measurements in real time, three maps are computed, having range and angle as the main axes. These maps are calculated with the first three spectral moments (respectively the CNR, the velocity centroid, and the velocity dispersion). The CNR map is useful for the lidar alignment setting and focus adjustments. The velocity map gives the position and trajectory of the vortex cores. The dispersion map provides information about wind turbulence.

Figure 11 shows a capture of the real time display with a wake vortex pair 325 m away from the lidar. The Y-axis is the range in m from the lidar, and the X-axis is the index of the line of sight, linearly dependent on the scan angle. The scanner executes symmetric sawtooth trajectories so that the right hand side of the display roughly mirrors the left hand side. The color scale gives the velocity information (spectrum centroid value) on each point of the scan plane. The real time display does not provide information about the maximum velocity component in the spectra, related to the wake vortex circulation. However, the presence and position of a wake vortex are clearly visible on the velocity map: a wake vortex has a characteristic signature.

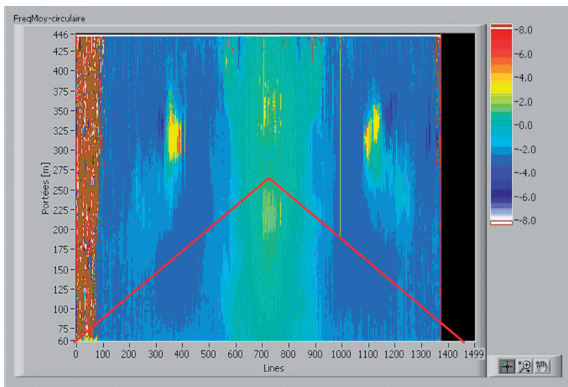


Figure 11 - Real time display of velocity map.

In order to determine the wake vortex age exactly, we installed a video camera, looking vertically above the Onera position, with a GPS time insert (see Figure 12). For each measurement, we know the time of the aircraft overflight.

The range resolution of 2.4 m is obtained by performing FFT analysis on 92 % overlapping 30 m-long gates (corresponding to the 200 ns pulse length); each gate is shifted by 2.4 m from the previous gate, as described by Köpp et al. [10]. The FFT spectral estimates are real time processed with DSP and displayed (Figure 11).



Figure 12 - Video recording for wake vortex aging.

The vortex velocity profiles are evaluated by searching for the maximal values (Figure 13, red line) and minimal values (Figure 13, blue line) in the frequency spectra of each range gate (Figure 13: each red line or blue line corresponds to one range gate).

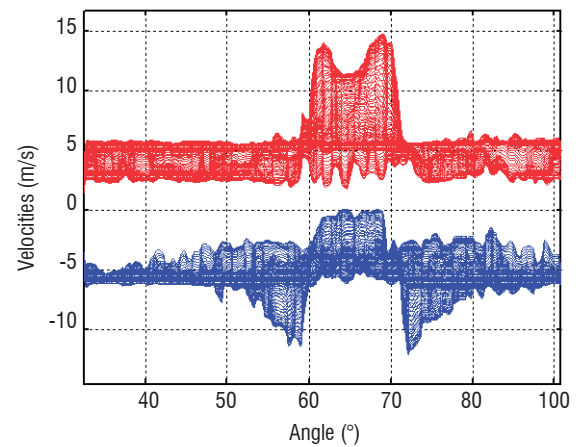


Figure 13 - Example of vortex spectra extraction from frequency spectra.

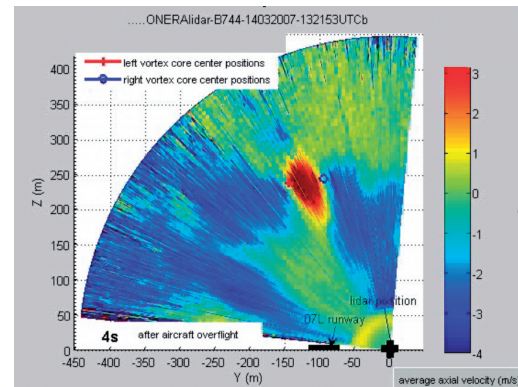


Figure 14 - Example of average velocity map display. The core positions are post processed. This shows the first measurement of a B747-400 on March 14th. This is a movie (Click on it to run).

The circulation is evaluated using the Smalikho method described in Köpp et al. [10]: the circulation is calculated by summation along an arc passing through the core center and between the radii 5 m and 15 m. The core position error is about ± 2 m and the circulation error is about 10 %.

Box 1 - Comparisons between lidar and PIV measurements

In the observation of vertical planes, transverse to the flight path of the model, PIV (particle imaging velocimetry) and lidar measurements allowed for tracking the wake vortex development in the B20 catapult facility, giving a more precise description of the secondary flow field as well as of the velocity profiles. Onera developed an innovative triangulation setup to obtain the vortex trajectory as a function of time. A PIV system, including several PIV cameras, was designed by DLR and Onera colleagues in the framework of the AWIATOR project; the evolution of the wake vortex could then be captured during a single shot. Catapult measurement results are presented in [13],[14] and [1]. During the AWIATOR project, PIV and lidar measurements were performed alternately, whereas during the DPAC project they were performed simultaneously on two different observation planes. They are complementary, since the first method allowed for detailed characterizations of the wake flow to ~ 40 wing spans behind the model (Figure B1-01), while the second one allowed for the tracking of vortices up to ~ 100 wing spans (Figure B1-02).

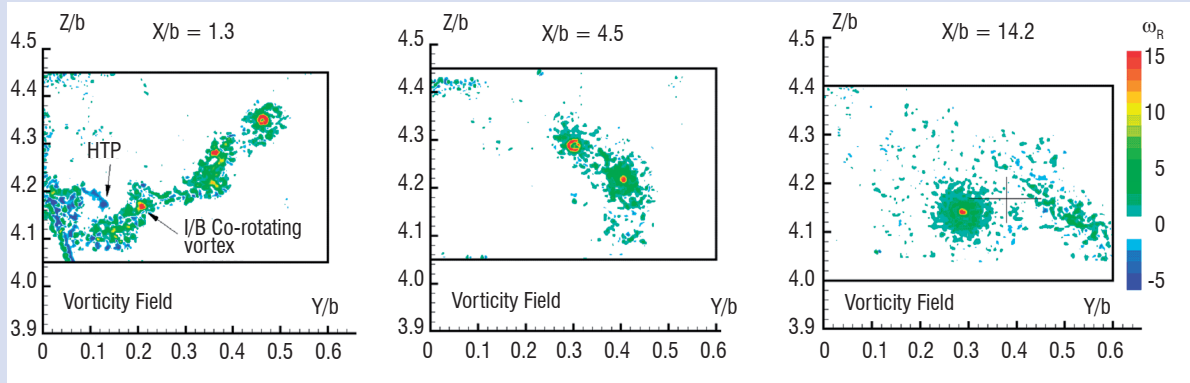


Figure B1-01 - Illustration of PIV measurements: Vorticity field recorded at different longitudinal locations X/b (four-engine type large aircraft model).

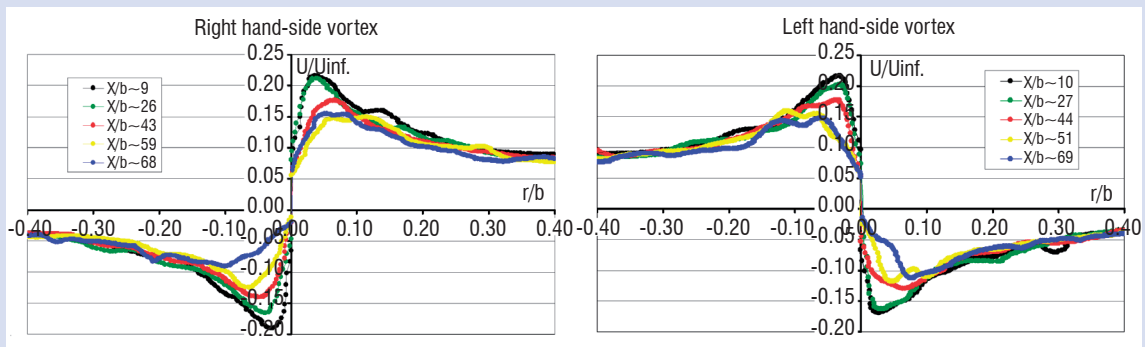


Figure B1-02 - Illustration of lidar measurements: Tangential velocity profiles recorded at different longitudinal locations X/b (generic very large transport-type aircraft model).

The PIV and lidar measurements are compared in Figure B1-03.

The velocity profile on the lidar line of sight is computed from the PIV velocity field and then compared with the results from the lidar measurements. In Figure 3, the lidar velocity profile is shown (in black) for $X/b \sim 10$, and the PIV velocity profile for $X/b \sim 8$ and $X/b \sim 12$. Although the PIV velocity maxima are slightly different from the lidar ones (because the vortex evolves from $X/b \sim 8$ to ~ 10 to ~ 12), the maxima are similar and the velocity profiles are very close.

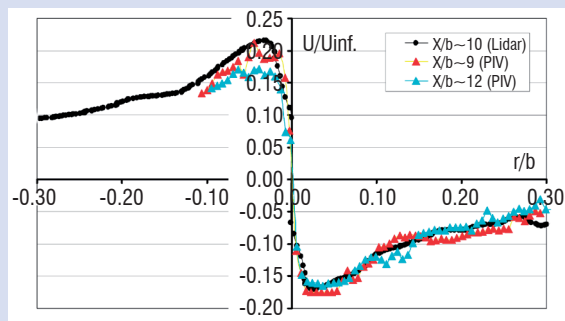


Figure B1-03 - Comparison between lidar and PIV measurements of tangential velocity profiles recorded at about the same longitudinal location (generic very large transport-type aircraft model)

The adequacy of lidar and PIV measurements has been demonstrated and the data provide mutual support for interpreting results.

Box 2 - Comparison between reduced-scale measurements and full-scale measurements

During the AWIATOR project, the wake vortex of a large transport aircraft-type configuration was characterized in the catapult facility with Onera's mini-lidar. This mini-lidar uses a 5W CW CO₂ laser, a transmitter-receiver telescope with a 1.5 cm objective lens and two 60 degree beam scanners, heterodyne coherent detection, and a triangulation technique. Measurements were obtained at high spectral frequency accuracy ($dV = 5$ cm/sec) and the precision of the core location was better than 15 cm.

Later, full-scale measurements were done at Tarbes airport by Onera's 10 μm CW lidar and DLR's 2 μm pulsed lidar. The pulsed lidar monitored the seeded vortices of a large transport aircraft (vortex position and circulation) while the CW lidar made detailed measurements of velocity profiles. During a previous EU project, CWAKE, an inter-comparison was already done for simultaneous wake vortex measurements by the DLR pulsed 2 μm lidar and two triangulating 10 μm CW lidars, one from QinetiQ and one from Onera. This CW Onera lidar used a 5W continuous wave CO₂ laser, a transmitter-receiver telescope with a 30 cm diameter aperture and a 50 degree beam scanner, and heterodyne coherent detection. The spectral resolution was $dV = 5$ cm/sec and the angular resolution was 2.2 mrad.

In order to compare reduced-scale and full-scale measurements, we normalized the parameters as suggested by T. Gertz et al. [1]. The evolution of the wake field behind an aircraft is usually described by the longitudinal distance X , normalized by $b/2$ (half the geometrical wing span):

$$X^* = X / (b / 2).$$

$X=0$ refers to the trailing edge of the wing tip, at a given value of the angle of attack or lift coefficient C_L .

Wake vortex evolution is usually plotted versus the dimensionless vortex lifetime t^* :

$$t^* = t / t_0,$$

where $t_0 = 2\pi b_0^2 / \Gamma_0$. Here b_0 is the initial vortex spacing after roll-up; $b_0 = s \cdot b$ (s , the spanwise load factor, is equal to $\pi/4$ for an elliptically loaded wing), and Γ_0 is the reference circulation.

$\Gamma_0 = C_L V_0 b / (2s \cdot A_R)$ is expressed in terms of lift coefficient C_L , aircraft or model speed V_0 , wingspan b and reference wing aspect ratio $A_R (= b^2 / S_{ref})$. S_{ref} is the wing reference surface.

The vortex velocity profiles are normalized by the aircraft or model speed V_0 :

$$V^* = V / V_0$$

Table 1 below compares experimental normalized resolutions of reduced-scale measurements at the catapult and airfield measurements.

| | Reduced-scale measurement | Full-scale measurement |
|--|---------------------------|------------------------|
| Normalized velocity resolution: dV / V_0 | 0.002 | 0.0006 |
| Normalized spatial resolution: $dx / (b / 2)$ | 0.015 | 0.015 |
| Normalized temporal resolution T / t_0 (T = time between two full vortex measurements) | 0.21 | 0.28 |

Table 1 - Experimental normalized resolutions of reduced-scale measurements at the catapult and field measurements

Only flights with the same wing configuration (reference configuration) can be compared. For the B20 tests, flights 9, 10 and 23 of the second campaign were in the reference configuration; for the Tarbes experiments, flights 1-13, 2-07 and 2-10 were in the reference configuration.

Figure B2-01 and Figure B2-02 provide examples of wake vortex trajectories measured by the DLR pulsed lidar for field measurement, and by the self-triangulation mini CW lidar for catapult measurement.

Whereas for field measurement the vortex trajectories are strongly driven by local wind and turbulence, the main left and right vortices generated downstream from the aircraft model descend uniformly in the catapult facility, disturbed only by local indoor turbulence. It is therefore easier to analyze wake vortex velocity profiles and temporal evolution in the catapult facility.

Figure B2-03 and Figure B2-04 give examples of velocity profile evolution, for field and catapult measurements respectively. Velocity profiles obtained in field measurements are smoother than catapult measurements because of the averaging of 100 spectra, despite a better normalized velocity resolution for the catapult data. Maximum tangential velocity peaks are higher for catapult measurement because of the better signal to noise ratio due to seeding. Nevertheless, reduced-scale and full-scale velocity profiles as well as the evolution in distance (or time) are in very good agreement.

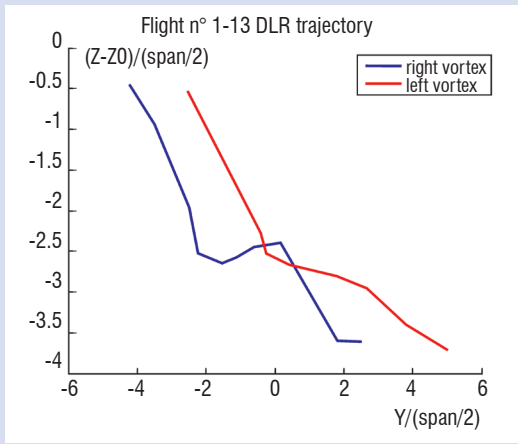


Figure B2-01 - Field test wake vortex measurements: left and right vortex trajectories measured by the 2 μm pulsed DLR lidar

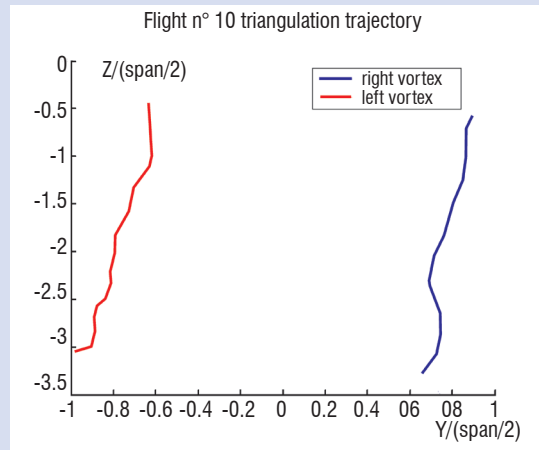


Figure B2-02 - Catapult (reduced-scale) vortex measurements: left and right vortex trajectories measured with self-triangulation CW mini-lidar.

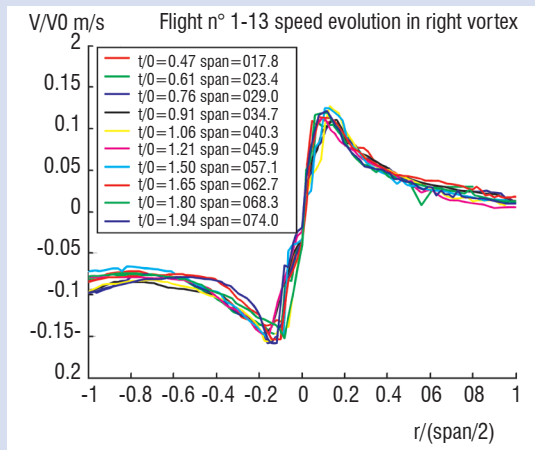


Figure B2-03 - Field test wake vortex measurements with Onera CW lidar: normalized velocity profile evolution.

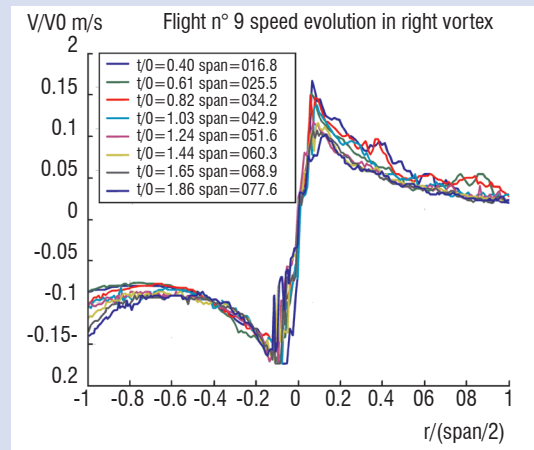


Figure B2-04 - Catapult (reduced-scale) vortex measurements with CW mini-lidar: normalized velocity profile evolution.

Figure B2-05 29 and Figure B2-06 give examples of circulation evolution, for field and catapult measurements respectively. Flight 2-07 took place in very quiet atmospheric conditions so the circulation decay was very low, and identical for both vortices. It fits very well with the circulation evolution in the catapult up to $t^* = 2$. After $t^* = 2$, at the catapult, the two vortices become unsymmetrical and their circulations differ.

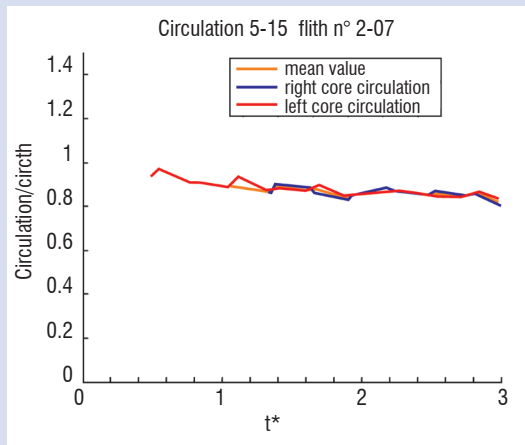


Figure B2-05 - Field test wake vortex measurements with Onera CW lidar: normalized circulation evolution.

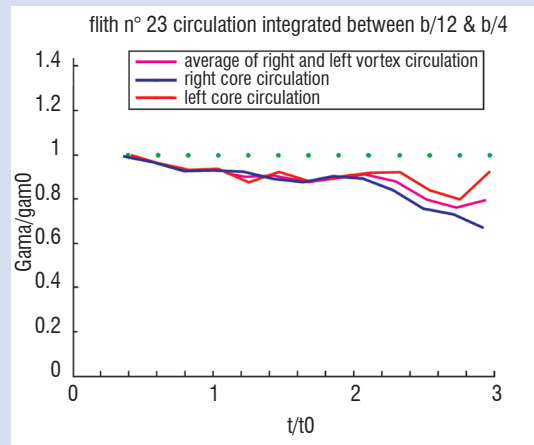


Figure B2-06 - Catapult (reduced-scale) vortex measurements with CW mini-lidar: normalized circulation evolution.

The scale factors between the model and true aircraft have been checked, and normalized results for reduced and full-scale measurements are in very good agreement. Lidar is the link between reduced-scale and full-scale approaches. Reduced-scale measurements are easier, cheaper and well-suited for fundamental research on aircraft configuration and devices. Full-scale measurements are however necessary to check the atmospheric impact on wake vortex evolution.

Figure 14 show examples of average velocity map displays for the first and last measurements of a B747-400 overflight on March 14th 2007. The core positions are post processed. Figure 15 displays the results from the measurements shown in Figure 14.

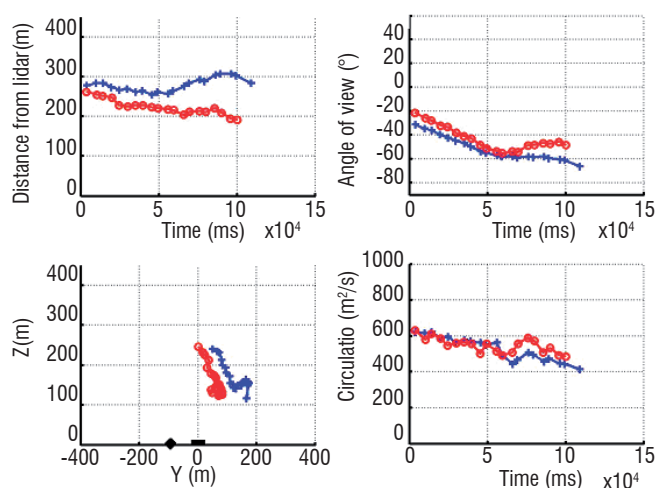


Figure 15 - Top left: distance of vortex cores from the lidar as a function of time after overflight (t.a.o.); top right: angle of view of vortex core as a function of t.a.o.; bottom left: vortex core trajectories in the measurement plane; bottom right: circulation values of left and right cores as functions of t.a.o.

Measurements of 187 departures at Frankfurt were obtained in only 8 days.

No particular effort was made to reduce the lidar size and there is still room for further reduction. This campaign proved that the fibered technology is now reliable and mature and little effort should be required to build a fully automatic system. Thanks to the good optical efficiency of fibered lasers, a fully autonomous temperature regulated system should require less than 500 W electrical power. The next steps are the size reduction and the automation of the lidar system.

Axial wake vortex detection

The purpose of the FIDELIO European project is to introduce a unique fiber laser technology geared for the aerospace industry requirements, enabling onboard realization of an atmospheric hazard detection lidar system. The FIDELIO lidar measures wind tracer velocities using coherent detection and a fiber architecture based on mainstream telecommunications components. The goal is to detect wake vortices along their axis at a range of 2 km.

In-flight demonstration of axial wake vortex detection was done during the IWAKE UE program [11].

FIDELIO project activities encompass the fiber laser design, the lidar simulations and design, and the field tests at Orly airport. A detailed presentation is available in [12].

Simulations

During FIDELIO, extensive simulation has been performed in order to specify an adequate laser. Onera has developed an end-to-end simulation tool including the observation geometry, the wake vortex velocity image, the scanning pattern, the lidar instrument, the wind turbulence outside the vortex, and the signal processing. A simulation

of large aircraft wake vortex evolution in a turbulent atmosphere has been performed by UCL/TERM.

The simulation's main conclusion is that the pulse duration must be at least 800ns. A 1600 ns pulse gives very good simulation results but was not chosen for the lidar design because such a large range gate (240m) would lead to a system sensitive to wind gradient.

Extensive simulations were carried out with varying laser energy E , pulse duration, PRF, and turbulence strength. The main conclusions are:

- At medium range ($>1\text{km}$), the vortex is easier to detect by measuring the spectrum broadening. These results confirm the IWAKE conclusions. [11]
- Longer pulse duration (800 ns) gives better results than the nominal value of 400 ns and leads to a high velocity resolution.
- The vortex is easier to detect at old ages than at young ones, since dissipation increases the velocity dispersion on the observation axis.
- Low PRF cannot be compensated for by increasing the laser energy. Indeed a high PRF value enables incoherent summation, reduced speckle effects and therefore a better velocity resolution.
- For PRF = 4 kHz, $E = 1\text{ mJ}$, and nominal atmospheric conditions the theoretical lidar range is 2400 m. For PRF = 10 kHz and $E = 0.1\text{ mJ}$, the theoretical lidar range is 1200 m.

Lidar architecture

Within FIDELIO, an innovative high-brightness pulsed $1.5\ \mu\text{m}$ laser source was built, based on a MOPFA architecture with a large core fiber. The beam quality is excellent ($M^2 = 1.3$). The pulsed energy achieved is $120\ \mu\text{J}$ with a PRF of 12 kHz and a pulse duration of 800 ns. With a further amplification stage, $750\ \mu\text{J}$ pulses were obtained in Onera lab at 5 kHz and $1\ \mu\text{s}$ with excellent beam quality. This last prototype has not been integrated in the field test.

The lidar optical architecture developed at Onera has the same base as SWAN, except for the larger output optic in order to focalize at 800 m.

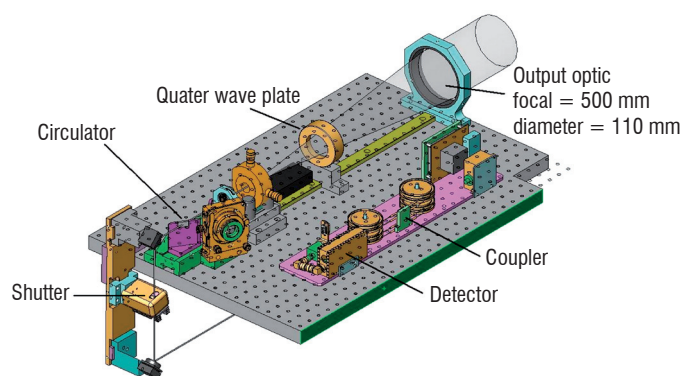


Figure 16 - Lidar optical layout.

The lidar includes a real-time display of the wind field, developed by UCL. Wind dispersion is post-processed.

Field tests

Field tests were carried out at Orly airport in April 2008. The lidar was placed about 800 m in front the runway touchdown threshold, facing the landing aircraft. The scanning configuration is presented in Figure 17. The total field of view is 12° horizontal \times 3° vertical. The image resolution was set to 128×32 pixels, giving an angular resolution of 1.6 mrad.

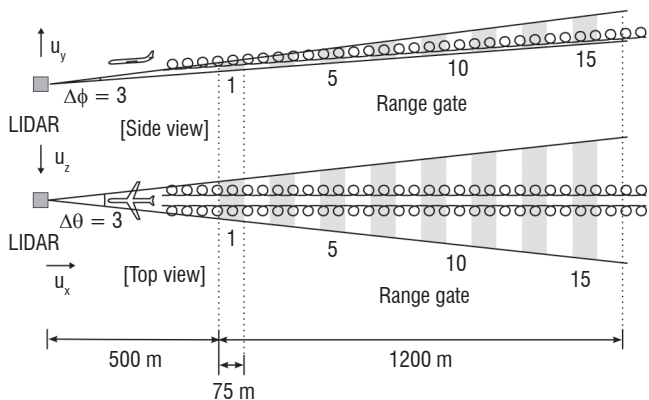


Figure 17 - Scanning configuration.

The overall average wind velocity displayed in the main window was validated with the atmospheric information coming from the tower.

In order to validate the vortex detection, video recordings were made of the landing aircraft during the test campaign. A real-time aircraft detection, tracking and geometric reconstruction algorithm was used to track the distance between the aircraft and the sensor.

Figure 18 shows a set of wind velocity dispersion images computed after the passing of two successive aircraft. Each box represents the 12° x 3° field of view image acquired at different ranges (vertical axis) and at different times (horizontal axis). We can clearly see the vortex signatures in scans 0 and 1 for the first plane and in scans 4 and 5 for the second one. The time elapsed between two scans is 6 seconds. The disappearance of the turbulence is mainly due to the lateral wind, which blows the vortices outside of the spatial region of scan. The distance from the vortex signature corresponds to the distance between the aircraft and the sensor as measured by the video detection and tracking system.

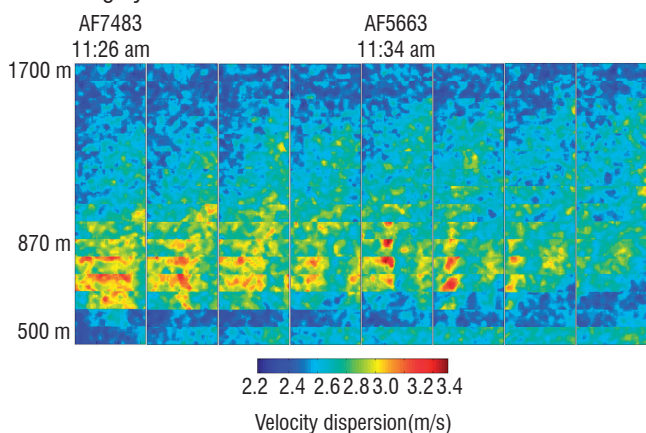


Figure 18 - Velocity dispersion images, calculated by UCL, obtained for 8 successive scans of 16 range gates of 75m after the passing of two successive aircraft. Each box represents the 12° x 3° field of view image acquired at different ranges (vertical axis) and at different times (horizontal axis).

Figure 19 and Figure 20 show a 3D representation of wake vortex detection on two consecutive scans a few seconds after a B747 landing. Each rectangle corresponds to a range gate. The X-axis represents the 12° horizontal field of view, the Z-axis the 3° vertical field of view and the Y-axis the distance of the range gates from the lidar. The detection was possible because the wind velocity showed strong discontinuities. The blue regions (gates 7 to 10 around 1.2km) are

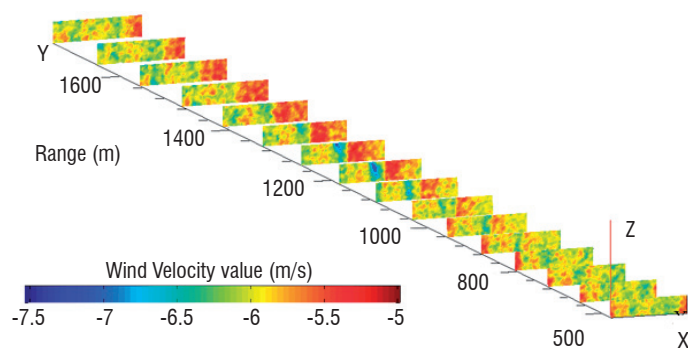


Figure 19 - 3D view of mean velocity images, calculated by UCL, obtained during the landing of a B747. (X axis = azimuth scan, Y axis = 16 range gates, and Z axis = elevation scan; color chart = line-of-sight wind speed).

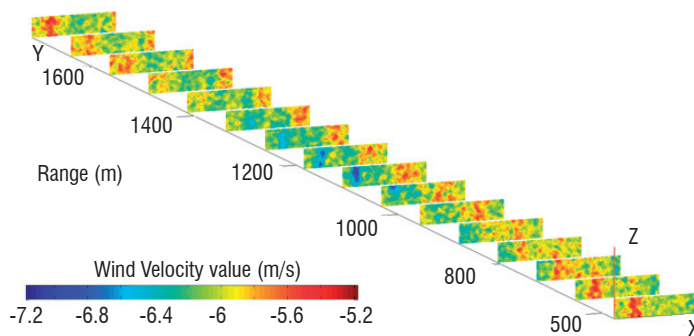


Figure 20 - 3D view of mean velocity images calculated by UCL, obtained during landing of a B747 (Xaxis = azimuth scan, Y axis = 16 range gates, and Z axis = elevation scan; color chart = line-of-sight wind speed).

again consistent with the aircraft location. We can see the wake vortex decay on the two consecutive scans. This range detection is in accordance with the simulated results.

This work was undertaken in the FIDELIO program and aims at meeting commercial aircraft requirements for onboard implementation of a wake vortex sensor. Among its results, the project has generated important advances in research and development on fiber laser technology.

Conclusions

For ten years now, Onera has been developing lidar tools for wake vortex detection and studies. Since 2003, new developments based on 1.5 μm fiber laser sources have been achieved, in parallel with extensive work on the laser sources themselves leading to breakthrough achievements. Recently three innovative lidars have been developed:

- 1) A mini-lidar with a CW 2W 1.5 μm laser source for aircraft model wake vortex characterization in the catapult facility. A self-triangulation technique allows for core location with 10cm precision and circulation estimation with 10% error.
- 2) A pulsed 1.5 μm lidar based on a 50 μJ / 15 kHz MOPA source for lateral wake vortex monitoring at airport sites. The range is 400 m, the core position error is about ± 2 m, and the circulation error is about 10 %.
- 3) A pulsed 1.5 μm lidar based on a 120 μJ / 12 kHz MOPA source for onboard axial wake vortex detection. The ground-based lidar test at Orly airport has demonstrated wake vortex detection up to 1.2 km. Our 1.5 μm fiber laser research continues and aims at increasing the laser source brightness and the lidar detection range for applications 2 and 3 ■

Acknowledgments

This work was supported by the European Union under grant No. 30837 (CREDOS) and grant No. 12008 (FIDELIO) and by DPAC-SPAé (Service Technique des Programmes Aéronautiques). The work presented in the inserts was supported by the European Union through the AWIATOR and CWAKE projects.

The authors thank Eric Coustols from Onera in Toulouse for the coordination of wake vortex research at Onera, and Frederic Moens from Onera in Meudon for the analysis of the PIV measurements.

The authors thank Thomas Peschel from the Fraunhofer Institute for lending the scanner in the FIDELIO project.

Thanks also to the FIDELIO project partners: ELOP (Israel, coordinator, laser integration), Thales R&T (France, laser research), INESC Porto (Portugal, laser research), IPHT (Denmark, fiber research and design), CeramOptec (Denmark, fiber packaging) and Thales Avionics (France, aircraft integration specifications).

References

- [1] T. GERTZ, F. HOLZÄPFEL and D. DARRACQ - *WakeNet Position Paper on Aircraft Wake Vortices*. European Union, April 2001.
- [2] S. M. HANNON and J. A. THOMSON - *Aircraft Wake Vortex Detection and Measurement with Pulsed Solid-State Coherent Laser Radar*. J Modern Opt, vol.41 (1994), p. 2175.
- [3] S. RAHM, I. SMALIKHO and F. KÖPP - *Characterization of Aircraft Wake Vortices by Airborne Coherent Doppler Lidar*. Journal of aircraft, vol. 44, no3, 2007, pp. 799-805
- [4] R. HEINRICHS, T. DASEY, M. MATTHEWS, S. CAMPBELL, R. FREEHART, G. PERRAS, and P. SALAMITOU - *Measurements of Aircraft Wake Vortices at Memphis International Airport with a cw CO₂ Coherent Laser Radar*. Proc. SPIE 2737, 122 (1996)
- [5] M. HARRIS, R. I. YOUNG, F. KÖPP, A. DOLFI, JP. CARIOU - *Wake Vortex Detection and Monitoring*. Aerospace Science and Technology, Volume 6, Issue 5, September 2002, Pages 325-331.
- [6] K. ASAKA, S. KAMEYAMA, T. ANDO, Y. HIRANO, H. INOKUCHI, and T. INAGAKI - *A 1.5 μ m all-Fiber Pulsed Airborne Doppler Lidar System*. JAXA IS17-06, (2003).
- [7] J.-P. CARIOU, B. AUGÈRE, D. GOULAR, J.-P. SCHLOTTERBECK and X. LACONDAMINE - *All-Fiber 1.5 μ m CW Coherent Laser Anemometer DALHEC. Helicopter Flight Test Analysis*. 13th Coherent Laser Radar conference (CLRC), Kamakura (2005).
- [8] F. KÖPP, I. SMALIKHO, S. RAHM, A. DOLFI, J.-P. CARIOU, M. HARRIS, R. I. YOUNG, K. WEEKES and N. GORDON - *Characterization of Aircraft Wake Vortices by Multiple-Lidar Triangulation*. AIAA Journal, vol. 41, no. 6 (June 2003), pp. 1081-1088.
- [9] G. CANAT, L. LOMBARD, S. JETSCHKE et al. - *Er-Yb-Doped LMA Fiber Structures for High Energy Amplification of Narrowlinewidth Pulses at 1.5 μ m*. Talk CtuBB, Conf. on Lasers and Electro-Optics (CLEO), Baltimore (2007).
- [10] S. M. HANNON and J. ALEX THOMSON - *Real Time Wake Vortex Detection, Tracking and Strength Estimation with Pulsed Coherent Lidar*. Proceedings of the 9th Conference on Coherent Laser Radar, June 23-27, 1997, Linköping, Sweden.
- [11] F. KÖPP, S. RAHM and I. N. SMALIKHO - *Characterization of Aircraft Wake Vortices by 2- μ m Pulsed Doppler Lidar*. Journal of Atmospheric and Oceanic Technology, vol. 21 (2004), pp. 194-206.
- [12] D. DOUXCHAMPS, Y. VERSCHUEREN, S. LUGAN, L. MUTUEL, B. MACQ and K. CHIHARA - *On-Board Axial Detection of Wake Vortices Using a 2 μ m Lidar*. IEEE Trans. on Aerospace and Electronic Systems, vol. 44, No. 4 (2008).
- [13] A. DOLFI-BOUTEYRE, G. CANAT, M. VALLA, B. AUGÈRE, C. BESSON, D. GOULAR, L. LOMBARD, J.-P. CARIOU, A. DURECU, D. FLEURY, L. BRICTEUX, S. BROUSMICHE, S. LUGAN and B. MACQ - IEEE jstqe, vol. 15, no 2, march/april 2009.
- [14] E. COUSTOLS, E. STUMPF, L. JACQUIN, F. MOENS, H. VOLLMERS and T. GERZ - *Minimised Wake: a Collaborative Research Programme on Aircraft Wake Vortices*. AIAA Paper 2003-0938, 41st Aerospace Sciences Meeting & Exhibit, Reno, NV, USA, 6-9 January 2003.
- [15] E. COUSTOLS, L. JACQUIN, F. MOENS and P. MOLTON - *Status of Onera Research on Wake Vortex in the Framework of National Activities and European Collaboration*. European Congress on Computational Methods in Applied Sciences and Engineering, ECCOMAS 2004 Conference, Jyväskylä, Finland, 24-28 July 2004 (P. Neittaanmäki, T. Rossi, S. Korotov, E. Oñate, J. Périaux and D. Knörzer, eds).
- [16] E. COUSTOLS, L. JACQUIN and G. SCHRAUF - *Status of Wake Vortex Alleviation in the Framework of European Collaboration: Validation Attempts Using Tests and CFD Results*. European Conference on Computational Fluid Dynamics, ECCOMAS CFD 2006 (P. Wesseling, E. Oñate and J. Périaux, eds).
- [17] C. BROSSARD, J.-C. MONNIER, PH. BARRICAU, F.-X. VANDERNOOT, Y. LE SANT, F. CHAMPAGNAT, G. LE BESNERAIS - *Principles and Applications of Particle Image Velocimetry*. AerospaceLab N°1, October 2009.

Acronyms

MOPA (Master Oscillator Power Amplifier)

LIDAR (Light Detection And Ranging)

CW (Continuous-Wave)

PIV (Particle Imaging Velocimetry)

MOPFA (Master Oscillator Power Fiber Amplifier)

HMI (Human-Machine Interface)

SBS (Stimulated Brillouin Scattering)

LMA (Large-Mode-Area)

ASE (Amplified Spontaneous Emission)



Agnès Dolfi-Bouteyre graduated from the «Ecole Supérieure d'Optique», Orsay, (1986) and received a PhD degree in Physics from University Paris XI Orsay (1990). She joined Onera in 1990 where she has been involved in the development of lidar systems for defense and aerospace.



Béatrice Augere has a PhD in non-linear optics (1988). She has been working at Onera since 1989 and is a research scientist in the "Lasers and Optoelectronics" research Unit. Her major research interests are lidars, laser propagation in turbulent flows and coherent detection.



Matthieu Valla received engineering and PhD degrees from Telecom Paristech (Paris, France) in 2001 and 2005. He has been working as a research engineer at Onera since 2002.



Didier Goular received a degree in electrical engineering from CNAM in 1990. Since 1985 he has been with the Onera Lidar team working on optimization of electronic and informatics processing of coherent optical systems.



Didier Fleury received an engineering degree in Physics and Metrology from DPE. He is currently working with the Onera Lidar team in SLS Unit.



Guillaume Canat graduated from the Ecole Polytechnique, Palaiseau (2000). He did his PhD thesis at the Ecole Nationale Supérieure de l'Aéronautique et de l'Espace in 2006. He has been a research scientist at Onera since 2002. His research interests include high-power fiber laser sources, non-linear effects in fibers and coherent combining.



Christophe Planchat has been working at Onera, on the optimization of electronics and informatics processing of coherent optical systems in the Optics Department, since 1991.



Thierry Gaudo has obtained his engineering degree from the «Conservatoire National des Arts et Métiers» (CNAM) in 1991. He has been involved in various LIDAR projects for defense or aerospace.



Claudine Besson obtained her PhD in Physics in 1989 at Optics Graduate School. She is a senior scientist and SLS group leader at Onera. Her current fields of interest are Fiber lasers and Lidars.



Anne Gilliot received the VKI Diploma in 1990 and her doctorate in Mechanics in 1997 from the University of Lille. Since 1991 she has been employed as a scientist by Onera and has taught Fluid Mechanics and Turbomachinery in engineering schools. She started with experimental work on problems of Fundamental Fluid Mechanics. Now she is working mainly on the development of Particle Image Velocimetry (PIV) and its use in aerodynamic applications and in large industrial scale wind tunnels in the PIV team of Applied Aerodynamics Department.



Jean-Pierre Cariou received an engineering degree in Optics from the "Ecole Supérieure d'Optique" in Orsay and a PhD in Astronomy and Spatial Techniques in 1983. At Onera, he has been involved in coherent lidars and laser imagers. He led the Laser and Optoelectronics research group for 10 years and was then special adviser for laser applications in the Optics Department. He joined the Leosphere company in 2007 as Technical Director, developing commercial wind and aerosol lidars for atmospheric applications.



Olivier Petilon graduated from 'ENSEA (Ecole Nationale Supérieure de l'Electronique et de ses Applications) (1992). From 1994 to 2001, he was Research and Development engineer for Electrocardiograms Analysis at Novacor, and from 2001 to 2002 Project Manager for Image processing at Poséidon-Technologie / Vision-IQ. He is currently Software Team Manager for Lidar Analysis at Leosphere. He is also the developer of Midizen software for music analysis (detection and recognition of pitches by fft algorithms).



Julius Lawson Daku received a M.Sc. degree in Physics («Magistère de Physique») from Université Paris 7 in 1993 and a M.Sc. degree in matter-radiation interaction («DEA Lasers et matière») from Université Paris 11 the same year. He received a PhD degree in Atom Optics from Université Paris 13 in 1997 and an M.Sc. degree in Computer Science from the CNAM in 2003. He is the technical director of the optoPartner company and a senior consultant for the company's partners and customers.



Sebastien Broumiche received an Electrical Engineering degree from the ECAM in 2002 and a DEA degree in electrical engineering from the Université Catholique de Louvain in January 2005. Since 2004, He has been a research engineer at the Communication and Remote Sensing Laboratory at the UCL. He is now working towards a PhD.



Sébastien Lugan received his master's degree and DEA in 2003 at the Ecole Supérieure d'Ingénieurs en Électronique et Électrotechnique (ESIEE), and the Gaspard-Monge Institute of Electronics and Computer Science, respectively. Since then, he joined the Communications and Remote Sensing Laboratory of the Université catholique de Louvain, where he is preparing a PhD thesis. His research interests include medical imaging, mega-image navigation and LiDAR detection of wake vortices.



Laurent Bricteux received his degree in mechanical engineering from the Université catholique de Louvain in 2000. Then, he worked for three years at LMS international as engineer in the field of numerical simulation of vibro-acoustic and aero-acoustic phenomena. In 2004 he joined the research group in Turbulence & Vortical flows held by Prof. G. Winckelmans. He received his ph.D degree from the Université catholique de Louvain in 2008. He is currently working on research projects in aeronautics and energetics.



Benoit Macq is currently a Professor at the University Catholique de Louvain in the Communication and Remote Sensing Laboratory.